# Fidelity Susceptibility Perspective on the Kondo Effect and Impurity Quantum Phase Transitions

Lei Wang,[1] Hiroshi Shinaoka,[1,2] and Matthias Troyer[1]
[1]Theoretische Physik, ETH Zurich, 8093 Zurich, Switzerland
[2]Department of Physics, University of Fribourg, 1700 Fribourg, Switzerland
(Received 3 August 2015; revised manuscript received 29 September 2015; published 1 December 2015)

The Kondo effect is a ubiquitous phenomenon appearing at low temperature in quantum confined systems coupled to a continuous bath. Efforts in understanding and controlling it have triggered important developments across several disciplines of condensed matter physics. A recurring pattern in these studies is that the suppression of the Kondo effect often results in intriguing physical phenomena such as impurity quantum phase transitions or non-Fermi-liquid behavior. We show that the fidelity susceptibility is a sensitive indicator for such phenomena because it quantifies the sensitivity of the system's state with respect to its coupling to the bath. We demonstrate the power of the fidelity susceptibility approach by using it to identify the crossover and quantum phase transitions in the one and two impurity Anderson models. The feasibility of measuring fidelity susceptibility in condensed matter as well as ultracold quantum gases experiments opens exciting new routes to diagnose the Kondo problem and impurity quantum phase transitions.

DOI: 10.1103/PhysRevLett.115.236601 PACS numbers: 72.10.Fk, 02.70.Ss, 05.30.Rt

The Kondo effect [1] was first observed in 1934 [2] as a low temperature resistance minimum in gold and was explained by Kondo in 1964 by taking into account the scattering of conduction electrons and magnetic impurities [3]. However, Kondo's perturbative calculation exhibits an unphysical divergence of the resistance at zero temperature. Resolving the Kondo problem has ultimately led to significant theoretical progress, including the formulation of the scaling laws [4], the development of the numerical renormalization group (NRG) method [5], and the application of phenomenological Fermi-liquid theory [6], Bethe ansatz [7,8], and boundary conformal field theory [9] to the quantum impurity problems. Experimental interest increased in the late 1990s due to breakthroughs in fabricating artificial nanodevices [10–15]. Kondo physics is also directly relevant to dissipative two-state systems [16] and the heavy-fermion compounds [17,18]. There has also been an increasing interest in realizing the Kondo effect in ultracold atomic gases [19–22]. High controllability of the latter system may offer chances to gain even deeper understandings of the intriguing physics of quantum impurity models.

A general description of the quantum impurity problems can be written as

$$\hat{H}(\lambda) = \underbrace{\hat{H}_{\text{impurity}} + \hat{H}_{\text{bath}}}_{\hat{H}_0} + \lambda \hat{H}_1, \tag{1}$$

where $\hat{H}_0$ describes the quantum impurity together with a continuous bath, and the last term describes the coupling between them. We treat $\lambda$ as a parameter and aim to characterize the state of the quantum impurity as a function of its coupling to the bath. The Kondo effect originates from the bath's tendency to screen the local moment formed on the quantum impurity. Renormalization group analysis shows that, in the Kondo region, the coupling strength flows to infinity at low energy [4,5], implying that the local moment will eventually get screened at a low enough temperature even with an arbitrarily weak bare impurity-bath coupling strength.

There are, however, various physical processes that can compete with the Kondo effect. In the presence of such competitions, the system may undergo an impurity quantum phase transition where a competing state (local moment, charge order, etc.) takes over as the bath-impurity coupling $\lambda$ decreases. Suppression of the Kondo screening often leads to non-Fermi liquid behavior [23,24]. However, different from the quantum phase transition in bulk systems [25], at such an impurity quantum critical point, only a nonextensive term in the free energy becomes singular. It is not always straightforward to find local probes to identify the impurity phase transitions. The question arises of how to diagnose and characterize such impurity quantum phase transitions in a general setting [26].

In this Letter, we argue that the fidelity susceptibility [27,28] provides a general and direct probe for an impurity quantum phase transition. The fidelity $F(\lambda_1, \lambda_2)$ of a quantum system is defined as the overlap of two ground state wave functions (or density matrices in the nonzero temperature case [29]) for coupling strengths $\lambda_1$ and $\lambda_2$. The fidelity susceptibility [27,28]

$$\chi_F(\lambda) = -\left.\frac{\partial^2 \ln F(\lambda, \lambda+\epsilon)}{\partial \epsilon^2}\right|_{\epsilon=0}, \tag{2}$$

 

typically exhibits a maximum at the phase boundary because the system's state changes drastically around the quantum critical point. Since it depends only on wave-function overlap but not on any local observable, fidelity susceptibility provides a natural way to diagnose a system irrespective of its specifics. Moreover, the fidelity susceptibility also fulfills the scaling laws [28,30]; thus, it is an effective tool for detecting and characterizing various quantum phase transitions, see Ref. [31] for a review.

Recently, some of us developed an efficient approach for calculating the fidelity susceptibility of quantum many-body systems [32] using modern quantum Monte Carlo (QMC) methods [33–43]. Specializing this to quantum impurity models, one can perform an expansion of the partition function at inverse temperature $\beta$ [44]

$$Z = \sum_{k=0}^{\infty} \lambda^k \int_0^\beta d\tau_1 \ldots \int_{\tau_{k-1}}^\beta d\tau_k \times \mathrm{Tr}[(-1)^k e^{-(\beta-\tau_k)\hat{H}_0} \hat{H}_1 \ldots \hat{H}_1 e^{-\tau_1 \hat{H}_0}]. \quad (3)$$

The Monte Carlo method can then be used to sample Eq. (3) and simulate quantum impurity models unbiasedly [45]. Equation (3) also provides a conceptual framework for understanding an impurity quantum phase transition through a quantum-classical mapping. The expansion can be formally interpreted as a grand canonical partition function of classical particles residing on a ring of length $\beta$. These particles represent the bath-impurity coupling events provided by the $\hat{H}_1$ terms, and their number is controlled by the coupling strength $\lambda$. Since Eq. (3) has the form of a fugacity expansion, an impurity quantum phase transition driven by $\lambda$ will manifest itself as a condensation phase transition of classical particles [48,49].

A concrete example of this general reasoning is provided by the Anderson-Yuval solution of the anisotropic Kondo model [50–53] with the Hamiltonian

$$\hat{H}_{\mathrm{Kondo}} = \sum_{\mathbf{k},\sigma} \epsilon_{\mathbf{k}} \hat{c}^\dagger_{\mathbf{k}\sigma} \hat{c}_{\mathbf{k}\sigma} + J_z \sum_{\mathbf{k},\mathbf{k}'} \hat{S}^z (\hat{c}^\dagger_{\mathbf{k}\uparrow} \hat{c}_{\mathbf{k}'\uparrow} - \hat{c}^\dagger_{\mathbf{k}\downarrow} \hat{c}_{\mathbf{k}'\downarrow}) + \lambda \sum_{\mathbf{k},\mathbf{k}'} (\hat{S}^+ \hat{c}^\dagger_{\mathbf{k}\downarrow} \hat{c}_{\mathbf{k}'\uparrow} + \mathrm{H.c.}). \quad (4)$$

The last term, which plays the role of $\lambda \hat{H}_1$ in Eq. (1), describes the coupling of the local impurity spin to free electrons in the bath through spin-flips. An expansion in the form of Eq. (3) and integration out of the free fermions lead to Anderson and Yuval's mapping of the Kondo model to a one-dimensional classical Coulomb gas [50]. As illustrated in Fig. 1(a), the spin flips can be interpreted as alternating positive and negative charges interacting through a logarithmic Coulomb potential [50–53]. The Coulomb gas picture provides an intuitive understanding of the Kondo effect and the renormalization group flow [51]. For a ferromagnetic coupling $J_z < 0$, the Coulomb gas exhibits

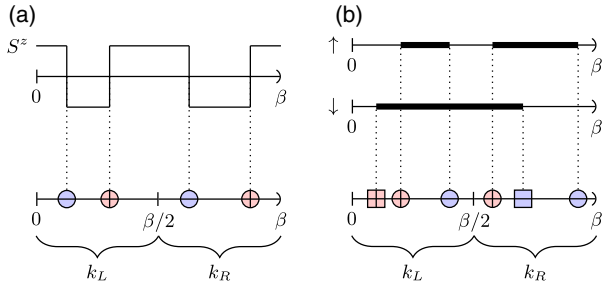


FIG. 1 (color online). (a) The Anderson-Yuval mapping of the Kondo model [Eq. (4)] to a one-dimensional classical Coulomb gas. The magnetization of the quantum impurity flips in the imaginary time due to the coupling to the bath. The spin flips can be interpreted as positive (red circles) and negative (blue circles) charges distributed on a periodic ring. (b) The continuous-time hybridization-expansion QMC algorithm, in the same spirit, maps the single impurity Anderson model [Eq. (6)] to a classical statistical problem. The thick segments indicate the occupation of the spin up and down impurity levels. The endpoints of each segment represent the hybridization events where the electrons hop in or out of the impurity, which are treated as classical objects in the QMC sampling. In both cases (a) and (b), the fidelity susceptibility is calculated as the covariance of $k_L$ and $k_R$, which count the number of bath-impurity coupling events in the two equal bipartitions of the imaginary-time axis.

a phase transition as the fugacity $\lambda$ changes. For small $\lambda < |J_z|$, these Coulomb charges are dilute and all associated in pairs, corresponding to the ferromagnetic Kondo state where the quantum impurity is spin polarized, while $\lambda > |J_z|$ corresponds to the antiferromagnetic Kondo state where the spin-flips are so frequent that the impurity shows no net magnetization; i.e., it is Kondo screened [54].

In the framework of Eq. (3), the fidelity susceptibility (2) can be readily calculated using a covariance estimator [32]

$$\chi_F = \frac{\langle k_L k_R \rangle - \langle k_L \rangle \langle k_R \rangle}{2\lambda^2}, \quad (5)$$

where $k_L$ and $k_R$ are the numbers of $\hat{H}_1$ operators in the two bipartitions of the imaginary-time axis. In the case of the Kondo model Eq. (4), they correspond to the number of Coulomb charges on either side of the bipartition, shown in the bottom of Fig. 1(a). It is clear from Anderson and Yuval's classical Coulomb gas picture that the fidelity susceptibility estimator (5) captures the critical fluctuation upon a condensation phase transition and, therefore, is able to signify the impurity phase transitions of the anisotropic Kondo model.

For general quantum impurity models, the estimator (5) quantifies the sensibility of the system's state with respect to the bath-impurity coupling and can, therefore, be used to diagnose impurity quantum phase transitions involving Kondo effects. Fidelity susceptibility is a generic probe of phase transition irrespective of details of the system [56].

Moreover, it can even be used to inspect the crossover physics, even though there is no sharp phase boundary [57].

As an illustration, first, we consider the single impurity Anderson model (SIAM) [58]

$$\hat{H}_{\mathrm{SIAM}} = \sum_{\mathbf{k},\sigma} \epsilon_{\mathbf{k}} \hat{c}^{\dagger}_{\mathbf{k}\sigma} \hat{c}_{\mathbf{k}\sigma} + \epsilon_d \sum_{\sigma} \hat{n}_{\sigma} + U \hat{n}_{\uparrow} \hat{n}_{\downarrow} + \lambda \sum_{\mathbf{k},\sigma} (\hat{c}^{\dagger}_{\mathbf{k}\sigma} \hat{d}_{\sigma} + \mathrm{H.c.}), \tag{6}$$

where $\hat{n}_{\sigma} = \hat{d}^{\dagger}_{\sigma} \hat{d}_{\sigma}$ is the impurity occupation number, and the second line describes the hybridization of the impurity and the noninteracting bath with strength $\lambda$. We consider a noninteracting bath with semicircle density-of-states $\rho(\epsilon) = \sum_{\mathbf{k}} \delta(\epsilon - \epsilon_{\mathbf{k}}) = \frac{2}{\pi D} \sqrt{1 - (\epsilon/D)^2}$ with $D = 2$ and choose $\epsilon_d = -U/2$ such that the model is at the particle-hole symmetric point. As we tune the on-site interaction $U$ and the hybridization strength $\lambda$, there is a crossover from a local moment regime, where the spin of the singly occupied impurity is effectively detached from the bath to the Kondo region, where the local moment is screened by the bath [59].

We use the continuous-time hybridization expansion algorithm [39] for our simulations and illustrate one Monte Carlo configuration in Fig. 1(b). Each dashed line indicates a hybridization event, where the electron hops on or off the impurity site, thus, changing the occupation (indicated by the thickness of the segments). The crossover from the local moment to the Kondo region is accompanied by the proliferation of the hybridization events in imaginary time. The fidelity susceptibility, Eq. (5), is easily measured by counting the number of hybridization events in a bipartition of the imaginary time axis, shown in the bottom of Fig. 1(b).

Figure 2(a) shows the fidelity susceptibility $\chi_F(\lambda)$ in the $U - \lambda$ plane with fixed inverse temperature $\beta = 100$ [60], where the peak indicates the crossover from local moment to Kondo region. This figure is a two-dimensional slice of the phase diagram of the Anderson impurity model sketched in the seminal NRG work of Ref. [59] (Fig. 12). The red solid line shows the contour determined by the Kondo temperature $1/\beta = T_K(U,\lambda) = \lambda\sqrt{U} e^{-\pi U/(8\lambda^2)}$ [61]. This boundary agrees with the maxima of the fidelity susceptibility, showing that it, indeed, correctly captures the crossover physics. The peak of fidelity susceptibility is higher at the small $\lambda$ region, which is a manifestation of the Anderson orthogonality catastrophe [62]: even a weak coupling to the quantum impurity drastically changes the state of the system.

To further confirm the relevance of the peak of the fidelity susceptibility, we calculate the local spin susceptibility

$$\chi_s = \int_0^{\beta} d\tau \langle \hat{S}^z(\tau) \hat{S}^z(0) \rangle, \tag{7}$$

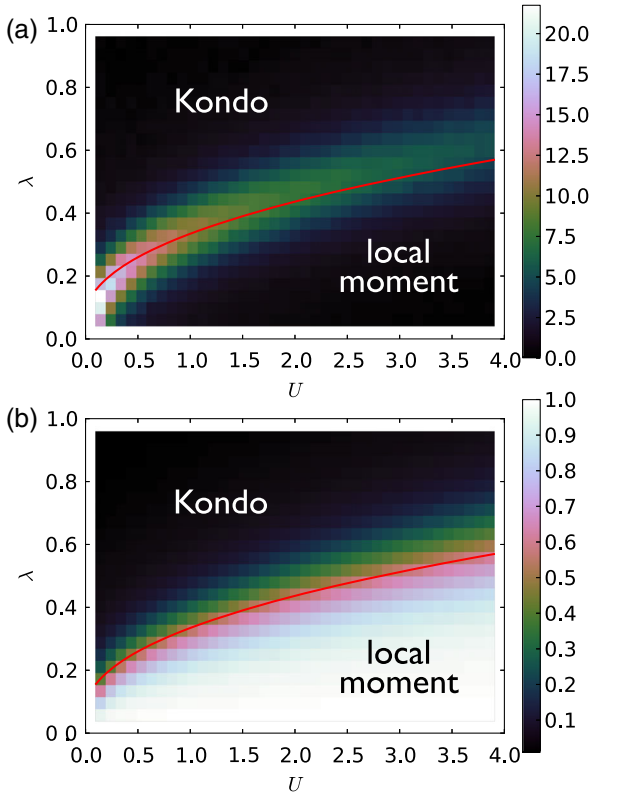


FIG. 2 (color online). Crossover from the local moment to the Kondo region in the single impurity Anderson model [Eq. (6)] revealed by (a) fidelity susceptibility and (b) spin susceptibility $4T\chi_s$ defined in Eq. (7). The red solid line shows the contour determined from the Kondo temperature $1/\beta = T_K(U,\lambda)$ [59,61].

where $\hat{S}^z = (\hat{n}_{\uparrow} - \hat{n}_{\downarrow})/2$ is the magnetization on the impurity. Figure 2(b) shows that $4T\chi_s$, which corresponds to the effective moment on the impurity, changes from one in the local moment region to zero in the Kondo region. The crossover region agrees with the peak determined from the fidelity susceptibility in Fig. 2(a).

As a second example, we consider the two-impurity Anderson model (TIAM) [63]

$$\hat{H}_{\mathrm{TIAM}} = \sum_{\mathbf{k},\alpha,\sigma} \epsilon_{\mathbf{k}} \hat{c}^{\dagger}_{\mathbf{k}\alpha\sigma} \hat{c}_{\mathbf{k}\alpha\sigma} + \epsilon_d \sum_{\alpha,\sigma} \hat{n}_{\alpha\sigma} + U \sum_{\alpha} \hat{n}_{\alpha\uparrow} \hat{n}_{\alpha\downarrow} + J \hat{\mathbf{S}}_1 \cdot \hat{\mathbf{S}}_2 + \lambda \sum_{\mathbf{k},\alpha,\sigma} (\hat{c}^{\dagger}_{\mathbf{k}\alpha\sigma} \hat{d}_{\alpha\sigma} + \mathrm{H.c.}), \tag{8}$$

where $\alpha = \{1, 2\}$ labels two impurity sites with occupation number $\hat{n}_{\alpha\sigma} = \hat{d}^{\dagger}_{\alpha\sigma} \hat{d}_{\alpha\sigma}$. The impurities have the same local interaction $U$ and on-site energy $\epsilon_d = -U/2$. Each impurity is coupled to its own bath with the hybridization strength $\lambda$. The second but last term represents the Ruderman-Kittel-Kasuya-Yosida (RKKY) [64–66] interaction between magnetic impurities in a metal. In the absence of this term, each impurity is Kondo screened by its own bath for the choice of $\lambda = 1$ and $\beta = 100$. However, the

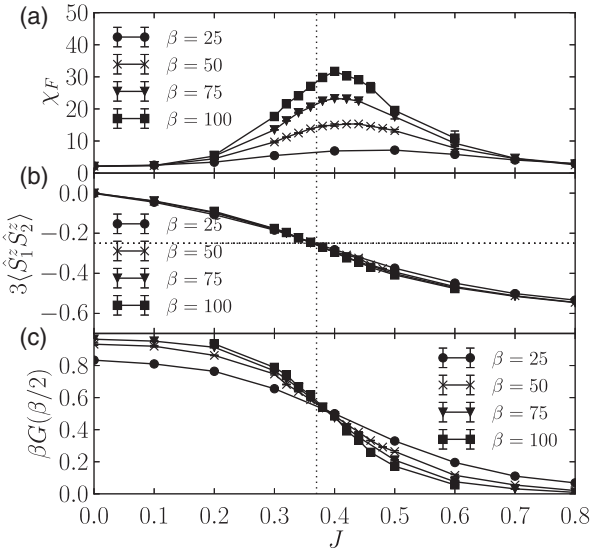


FIG. 3. (a) The fidelity susceptibility, (b) equal-time spin-spin correlation, and (c) density-of-states at the Fermi level of the two-impurity Anderson model Eq. (8) as a function of the interimpurity RKKY coupling strength. The dashed vertical line indicates the critical point $J_c = 0.37$ where the equal-time spin-spin correlation $3\langle \hat{S}_1^z \hat{S}_2^z \rangle = -0.25$ [68,73].

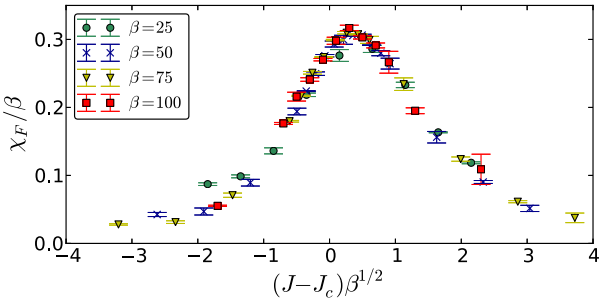


FIG. 4 (color online). Data collapse of the scaled fidelity susceptibility with $J_c = 0.37$. The data are the same as in Fig. 3(a).

antiferromagnetic RKKY coupling $J > 0$ favors a singlet formed between the two impurity spins, which competes with the Kondo screening and causes an impurity quantum phase transition [67,68]. Detailed studies of the two impurity Anderson (and Kondo) model have provided insights into various aspects of Kondo [69,70] and heavy fermion physics [71].

Simulation of the two impurity Anderson model (8) goes beyond the segment picture illustrated in Fig. 1(b), and thus, we adopt an algorithm [44,72] suitable for general interactions. The fidelity susceptibility is still calculated in the same way, by simply counting the number of hybridization events. As shown in Fig. 3(a), it exhibits an increasingly sharp peak as the inverse temperature $\beta$ increases. The peak location shifts towards the vertical dashed line, where the equal-time spin-spin correlation $\langle \hat{\mathbf{S}}_1 \cdot \hat{\mathbf{S}}_2 \rangle = 3\langle \hat{S}_1^z \hat{S}_2^z \rangle = -0.25$ in Fig. 3(b). According to previous NRG studies [68,73], the quantum critical point is right at the dashed line. Obviously, the fidelity susceptibility offers a better indication of the phase transition compared to the spin-spin correlations because the later quantity is featureless at the critical point and has much weaker temperature dependence. Figure 3(c) shows the density of states at the Fermi level, which decreases as the spin singlet state takes over the Kondo state in the large $J$ limit [74].

Next, we perform a scaling analysis of the fidelity susceptibility close to the quantum critical point [30]. Since an infinite bath was assumed, the only finite dimension is the inverse temperature. Figure 4 shows the scaled fidelity susceptibility $\chi_F/\beta$ versus $(J - J_c)\beta^{1/2}$ with $J_c = 0.37$, which results in a good data collapse. Although the scaling form is chosen empirically according to the one for lattice systems [30], the observed scaling exponents agree with the considerations of Ref. [75]. The observed data collapse suggests that the fidelity susceptibility not only captures the impurity quantum critical point, but also the values of the critical exponents, which are an indicator for the universality class of a quantum phase transition.

Our Letter shows that the fidelity susceptibility is a versatile tool for probing and inspecting phase transition and crossover physics in quantum impurity models. It is readily accessible in QMC simulations, and it serves as a general purpose indicator for the breakdown of the Kondo effect. Conceptually, our work exploits the intrinsic quantum to classical mapping of the quantum impurity models in the context of modern QMC approaches.

Recent experimental and theoretical studies explore an even richer variety of complex quantum impurities and phase transitions, such as the interplay of the Kondo effect and interimpurity couplings [76–78], coupling to superconducting or Dirac fermion baths [79–83], and the effect of multiple levels or multiple channels [84–87], see Refs. [24,88] for a review. The fidelity susceptibility will provide a valuable tool to discover rich physical phenomena in such settings. In a broader context, since much of the physics of quantum impurity models also manifest themselves in lattice models [89,90] through the dynamical-mean-field-theory framework [91,92], fidelity susceptibility of these auxiliary quantum impurity problems may shed light on phase transitions of correlated materials.

Finally, it is worth mentioning that fidelity susceptibility is related to the dynamical response of the $\hat{H}_1$ term that is measurable using either time-dependent ramps or quenches [93] or through spectroscopy measurements [94,95]. Alternatively, fidelity susceptibility can also be obtained from the overlap of quantum many-body wave functions, which has been measured in a NMR quantum simulator [96] and, notably, in ultracold bosons by utilizing a quantum gas microscope [97]. Combining these detection approaches with recent efforts of realizing Kondo physics in ultracold atomic gases [19–22], the proposed diagnostic

tool based on fidelity susceptibility would be useful in a real setting in the laboratory.

We thank Ralf Bulla, Ninghua Tong, and U.-J. Wiese for helpful discussions. Simulations were performed on the Mönch and Brutus clusters at ETH Zurich. We have used the ALPS HYBRIDIZATION application [98] and ALPS libraries [99] for our simulations and data analysis. This work was supported by the ERC Advanced Grant SIMCOFE, by the Swiss National Science Foundation through Grant No. 200021E-149122 and the National Centers of Competence in Research QSIT and MARVEL, and by the DFG via FOR 1346 and ERC Consolidator Grant CORRELMAT (Project No. 617196). M. T. acknowledges the hospitality of the Aspen Center for Physics, supported by NSF Grant No. PHY-1066293.

[1] A. C. Hewson, *The Kondo Problem to Heavy Fermions* (Cambridge University Press, Cambridge, England, 1997).
[2] W. J. de Haas, J. de Boer, and G. J. van dën Berg, Physica (Amsterdam) **1**, 1115 (1934).
[3] J. Kondo, Prog. Theor. Phys. **32**, 37 (1964).
[4] P. W. Anderson, J. Phys. C **3**, 2436 (1970).
[5] K. G. Wilson, Rev. Mod. Phys. **47**, 773 (1975).
[6] P. Nozieres, J. Low Temp. Phys. **17**, 31 (1974).
[7] P. B. Vigman, JETP Lett. **31**, 364 (1980).
[8] N. Andrei, Phys. Rev. Lett. **45**, 379 (1980).
[9] I. Affleck, Acta Phys. Pol. B **26**, 1869 (1995).
[10] L. Kouwenhoven and L. Glazman, Phys. World **14**, 33 (2001).
[11] L. I. Glazman and M. E. Raikh, JETP Lett. **47**, 452 (1988).
[12] T.-K. Ng and P. A. Lee, Phys. Rev. Lett. **61**, 1768 (1988).
[13] S. M. Cronenwett, T. H. Oosterkamp, and L. P. Kouwenhoven, Science **281**, 540 (1998).
[14] D. Goldhaber-Gordon, H. Shtrikman, D. Mahalu, D. Abusch-Magder, U. Meirav, and M. A. Kastner, Nature (London) **391**, 156 (1998).
[15] W. G. Van der Wiel, S. De Franceschi, T. Fujisawa, J. M. Elzerman, S. Tarucha, and L. P. Kouwenhoven, Science **289**, 2105 (2000).
[16] A. J. Leggett, S. Chakravarty, A. T. Dorsey, M. P. A. Fisher, A. Garg, and W. Zwerger, Rev. Mod. Phys. **59**, 1 (1987).
[17] Q. Si, S. Rabello, K. Ingersent, and J. L. Smith, Nature (London) **413**, 804 (2001).
[18] P. Gegenwart, Q. Si, and F. Steglich, Nat. Phys. **4**, 186 (2008).
[19] J. Bauer, C. Salomon, and E. Demler, Phys. Rev. Lett. **111**, 215304 (2013).
[20] Y. Nishida, Phys. Rev. Lett. **111**, 135301 (2013).
[21] B. Sundar and E. J. Mueller, arXiv:1503.05234.
[22] R. Zhang, D. Zhang, Y. Cheng, W. Chen, P. Zhang, and H. Zhai, arXiv:1509.01350.
[23] R. Bulla and M. Vojta, in *Concepts in Electron Correlation* (Springer, New York, 2003), pp. 209–217.
[24] M. Vojta, Philos. Mag. **86**, 1807 (2006).
[25] S. Sachdev, *Quantum Phase Transition* (Cambridge University Press, Cambridge, England, 2011).
[26] A. Bayat, H. Johannesson, S. Bose, and P. Sodano, Nat. Commun. **5**, 3784 (2014).
[27] W.-L. You, Y. W. Li, and S.-J. Gu, Phys. Rev. E **76**, 022101 (2007).
[28] L. Campos Venuti and P. Zanardi, Phys. Rev. Lett. **99**, 095701 (2007).
[29] J. Sirker, Phys. Rev. Lett. **105**, 117203 (2010).
[30] A. F. Albuquerque, F. Alet, C. Sire, and S. Capponi, Phys. Rev. B **81**, 064418 (2010).
[31] S.-J. Gu, Int. J. Mod. Phys. B **24**, 4371 (2010).
[32] L. Wang, Y.-H. Liu, J. Imriška, P. N. Ma, and M. Troyer, Phys. Rev. X **5**, 031007 (2015).
[33] A. W. Sandvik and J. Kurkijärvi, Phys. Rev. B **43**, 5950 (1991).
[34] B. B. Beard and U.-J. Wiese, Phys. Rev. Lett. **77**, 5130 (1996).
[35] N. V. Prokof'ev, B. V. Svistunov, and I. S. Tupitsyn, J. Exp. Theor. Phys. **87**, 310 (1998).
[36] H. G. Evertz, Adv. Phys. **52**, 1 (2003).
[37] N. Kawashima and K. Harada, J. Phys. Soc. Jpn. **73**, 1379 (2004).
[38] A. N. Rubtsov, V. V. Savkin, and A. I. Lichtenstein, Phys. Rev. B **72**, 035122 (2005).
[39] P. Werner, A. Comanac, L. de' Medici, M. Troyer, and A. J. Millis, Phys. Rev. Lett. **97**, 076405 (2006).
[40] E. Gull, P. Werner, O. Parcollet, and M. Troyer, Europhys. Lett. **82**, 57003 (2008).
[41] S. M. A. Rombouts, K. Heyde, and N. Jachowicz, Phys. Rev. Lett. **82**, 4155 (1999).
[42] M. Iazzi and M. Troyer, Phys. Rev. B **91**, 241118 (2015).
[43] L. Wang, M. Iazzi, P. Corboz, and M. Troyer, Phys. Rev. B **91**, 235151 (2015).
[44] E. Gull, A. J. Millis, A. I. Lichtenstein, A. N. Rubtsov, M. Troyer, and P. Werner, Rev. Mod. Phys. **83**, 349 (2011).
[45] The continuous-time hybridization expansion algorithm [39] solves (multiorbital) Anderson impurity models, while the algorithm of Ref. [46] is suitable for the Kondo model and its multiorbital generalization such as the Coqblin-Schrieffer model [47].
[46] J. Otsuki, H. Kusunose, P. Werner, and Y. Kuramoto, J. Phys. Soc. Jpn. **76**, 114707 (2007).
[47] B. Coqblin and J. R. Schrieffer, Phys. Rev. **185**, 847 (1969).
[48] C. N. Yang and T. D. Lee, Phys. Rev. **87**, 404 (1952).
[49] T. D. Lee and C. N. Yang, Phys. Rev. **87**, 410 (1952).
[50] P. W. Anderson and G. Yuval, Phys. Rev. Lett. **23**, 89 (1969).
[51] P. W. Anderson, G. Yuval, and D. R. Hamann, Phys. Rev. B **1**, 4464 (1970).
[52] K. Schotte, Z. Phys. **230**, 99 (1970).
[53] P. W. Anderson and G. Yuval, *Asymptotically Exact Methods in the Kondo Problem* (Academic Press, Inc., New York, 1973).
[54] Reference [55] performed one of the first historic Monte Carlo simulations of the Kondo model Eq. (4) based on the Coulomb gas analogy. However, the simulation was performed in a canonical ensemble with a fixed number of spin flips and, thus, has systematic errors in the high temperature region [53].
[55] K. D. Schotte and U. Schotte, Phys. Rev. B **4**, 2228 (1971).
[56] The singularity of the fidelity susceptibility upon a phase transition is also stronger than the second order derivative of the free energy (related to variance of the total expansion order) [30,32].

[57] A. Khan and P. Pieri, Phys. Rev. A **80**, 012303 (2009).
[58] P. W. Anderson, Phys. Rev. **124**, 41 (1961).
[59] H. R. Krishna-murthy, J. W. Wilkins, and K. G. Wilson, Phys. Rev. B **21**, 1003 (1980).
[60] See Supplemental Material at http://link.aps.org/supplemental/10.1103/PhysRevLett.115.236601 for the fidelity susceptibility data at various temperatures along a horizontal cut of Fig. 2(a) at $\lambda = 0.4$.
[61] F. D. M. Haldane, Phys. Rev. Lett. **40**, 416 (1978).
[62] P. W. Anderson, Phys. Rev. Lett. **18**, 1049 (1967).
[63] Y. Nishikawa, D. J. G. Crow, and A. C. Hewson, Phys. Rev. B **86**, 125134 (2012).
[64] M. A. Ruderman and C. Kittel, Phys. Rev. **96**, 99 (1954).
[65] T. Kasuya, Prog. Theor. Phys. **16**, 45 (1956).
[66] K. Yosida, Phys. Rev. **106**, 893 (1957).
[67] B. A. Jones and C. M. Varma, Phys. Rev. Lett. **58**, 843 (1987).
[68] B. A. Jones, C. M. Varma, and J. W. Wilkins, Phys. Rev. Lett. **61**, 125 (1988).
[69] I. Affleck, A. W. W. Ludwig, and B. A. Jones, Phys. Rev. B **52**, 9528 (1995).
[70] A. K. Mitchell, E. Sela, and D. E. Logan, Phys. Rev. Lett. **108**, 086405 (2012).
[71] P. Sun and G. Kotliar, Phys. Rev. Lett. **95**, 016402 (2005).
[72] P. Werner and A. J. Millis, Phys. Rev. B **74**, 155107 (2006).
[73] B. A. Jones and C. M. Varma, Phys. Rev. B **40**, 324 (1989).
[74] If there is a tunneling between the two impurities, the charge transfer will smear out the quantum phase transition into a crossover [75]. Even in this case, we still identify a peak in the fidelity susceptibility (not shown) that indicates the change of the system's state in the crossover region.
[75] G. Zaránd, C.-H. Chung, P. Simon, and M. Vojta, Phys. Rev. Lett. **97**, 166802 (2006).
[76] H. Jeong, A. M. Chang, and M. R. Melloch, Science **293**, 2221 (2001).
[77] D. E. Liu, S. Chandrasekharan, and H. U. Baranger, Phys. Rev. Lett. **105**, 256801 (2010).
[78] J. Bork, Y.-h. Zhang, L. Diekhöner, L. Borda, P. Simon, J. Kroha, P. Wahl, and K. Kern, Nat. Phys. **7**, 901 (2011).
[79] R. Maurand, T. Meng, E. Bonet, S. Florens, L. Marty, and W. Wernsdorfer, Phys. Rev. X **2**, 011009 (2012).
[80] H. T. Mebrahtu, I. V. Borzenets, D. E. Liu, H. Zheng, Y. V. Bomze, A. I. Smirnov, H. U. Baranger, and G. Finkelstein, Nature (London) **488**, 61 (2012).
[81] K. J. Franke, G. Schulze, and J. I. Pascual, Science **332**, 940 (2011).
[82] J.-H. Chen, L. Li, W. G. Cullen, E. D. Williams, and M. S. Fuhrer, Nat. Phys. **7**, 535 (2011).
[83] J.-D. Pillet, P. Joyez, R. Žitko, and M. F. Goffman, Phys. Rev. B **88**, 045101 (2013).
[84] R. M. Potok, I. G. Rau, H. Shtrikman, Y. Oreg, and D. Goldhaber-Gordon, Nature (London) **446**, 167 (2007).
[85] N. Roch, S. Florens, V. Bouchiat, W. Wernsdorfer, and F. Balestro, Nature (London) **453**, 633 (2008).
[86] X. Wang and A. J. Millis, Phys. Rev. B **81**, 045106 (2010).
[87] M. Goldstein, R. Berkovits, and Y. Gefen, Phys. Rev. Lett. **104**, 226805 (2010).
[88] I. Rau, S. Amasha, Y. Oreg, and D. Goldhaber-Gordon, in *Understanding Quantum Phase Transitions* (CRC Press, Boca Raton, FL, 2010), p. 341.
[89] R. Bulla, Philos. Mag. **86**, 1877 (2006).
[90] M. Ferrero, L. De Leo, P. Lecheminant, and M. Fabrizio, J. Phys. Condens. Matter **19**, 433201 (2007).
[91] A. Georges, G. Kotliar, W. Krauth, and M. J. Rozenberg, Rev. Mod. Phys. **68**, 13 (1996).
[92] T. Maier, M. Jarrell, T. Pruschke, and M. H. Hettler, Rev. Mod. Phys. **77**, 1027 (2005).
[93] M. Kolodrubetz, V. Gritsev, and A. Polkovnikov, Phys. Rev. B **88**, 064304 (2013).
[94] S.-J. Gu and W. C. Yu, Europhys. Lett. **108**, 20002 (2014).
[95] P. Hauke, M. Heyl, L. Tagliacozzo, and P. Zoller, arXiv:1509.01739.
[96] J. Zhang, X. Peng, N. Rajendran, and D. Suter, Phys. Rev. Lett. **100**, 100501 (2008).
[97] R. Islam, R. Ma, P. M. Preiss, M. E. Tai, A. Lukin, M. Rispoli, and M. Greiner, arXiv:1509.01160.
[98] H. Hafermann, P. Werner, and E. Gull, Comput. Phys. Commun. **184**, 1280 (2013).
[99] B. Bauer *et al.*, J. Stat. Mech. (2011) P05001.